



UNIVERSITY OF LEEDS

This is a repository copy of *Rapidly rotating Maxwell-Cattaneo convection*.

White Rose Research Online URL for this paper:

<https://eprints.whiterose.ac.uk/191716/>

Version: Accepted Version

Article:

Hughes, DW orcid.org/0000-0002-8004-8631, Proctor, MRE and Eltayeb, IA (2022) Rapidly rotating Maxwell-Cattaneo convection. *Physical Review Fluids*, 7 (9). 093502. ISSN 2469-990X

<https://doi.org/10.1103/PhysRevFluids.7.093502>

©2022 American Physical Society. This is an author produced version of an article published in *Physical Review Fluids*. Uploaded in accordance with the publisher's self-archiving policy.

Reuse

Items deposited in White Rose Research Online are protected by copyright, with all rights reserved unless indicated otherwise. They may be downloaded and/or printed for private study, or other acts as permitted by national copyright laws. The publisher or other rights holders may allow further reproduction and re-use of the full text version. This is indicated by the licence information on the White Rose Research Online record for the item.

Takedown

If you consider content in White Rose Research Online to be in breach of UK law, please notify us by emailing eprints@whiterose.ac.uk including the URL of the record and the reason for the withdrawal request.



eprints@whiterose.ac.uk
<https://eprints.whiterose.ac.uk/>

Rapidly rotating Maxwell-Cattaneo convection

D. W. Hughes,^{1,*} M. R. E. Proctor,² and I. A. Eltayeb³

¹*School of Mathematics, University of Leeds, Leeds LS2 9JT, UK*

²*DAMTP, Centre for Mathematical Sciences, Wilberforce Road, Cambridge CB3 0WA, UK*

³*The Faculty of Mathematical Sciences and Informatics,*

University of Khartoum, POB 321, Khartoum, Sudan

(Dated: September 9, 2022)

Motivated by astrophysical and geophysical applications, the classical problem of rotating Rayleigh-Bénard convection has been widely studied. Assuming a classical Fourier heat law, in which the heat flux is directly proportional to the temperature gradient, the evolution of temperature is governed by a parabolic advection-diffusion equation; this, in turn, implies an infinite speed of propagation of information. In reality, the system is rendered hyperbolic by extending the Fourier law to include an advective derivative of the flux — the Maxwell-Cattaneo (M-C) effect. Although the correction (measured by the parameter Γ , a non-dimensional representation of the relaxation time) is nominally small, it represents a singular perturbation and hence can lead to significant effects when the rotation rate (measured by the Taylor number T) is sufficiently high. In this paper, we investigate the linear stability of rotating convection, incorporating the M-C effect, concentrating on the regime of $T \gg 1$, $\Gamma \ll 1$. On increasing Γ for a fixed $T \gg 1$, M-C effects first come into play when $\Gamma = O(T^{-1/3})$. Here, as in the classical problem, the preferred mode can be either steady or oscillatory, depending on the value of the Prandtl number σ . For $\Gamma > O(T^{-1/3})$, the influence of the M-C effect is sufficiently strong that the onset of instability is always oscillatory, regardless of the value of σ . Within this regime, the dependence on σ of the critical Rayleigh number and of the scale of the preferred mode are explored through the analysis of specific distinguished limits.

I. INTRODUCTION

It has been noted by a number of authors that the classical Fourier law connecting heat flux and the gradient of temperature — leading to a parabolic equation for the spatiotemporal evolution of the temperature field — should be corrected to allow both for relativistic effects and to accommodate the processes in real materials that are responsible for heat transfer. Maxwell [1] proposed a modified equation for gases incorporating a finite relaxation time. Cattaneo [2] proposed a similar relation for solids. This was developed further by Oldroyd [3], and later contributions were made by Fox [4] and Carrassi and Morro [5]. These extensions are collectively referred to as the Maxwell-Cattaneo (M-C) effect. The M-C heat transport effect has been studied in a wide variety of different physical contexts: for example, in solids [6], in fluids [7–14], in porous media [15, 16], in nanofluids and nanomaterials [17–20], in liquid helium [21, 22], and in the physics of phase changes [23, 24]. The M-C effect has been shown to be of particular importance in a variety of biological systems [25–32]. It has also been modelled theoretically in various astrophysical contexts [33–35], as well as in the dynamics of traffic flow [36].

While the Fourier law can be written as $\mathbf{q} = -K\nabla T$, where \mathbf{q} is the heat flux, T is the temperature and K is the thermal conductivity, the M-C effect introduces a relaxation time τ , leading to the equation

$$\tau \frac{\mathcal{D}\mathbf{q}}{\mathcal{D}t} + \mathbf{q} = -K\nabla T, \quad (1)$$

where \mathcal{D} represents a generalised material derivative, chosen to give expressions that do not depend on the frame of observation. In the present paper, which discusses only linear stability considerations, almost all such choices give the same result. Further discussion of the choice of derivative can be found in refs. [37, 38].

The importance of the new time derivative term can be assessed by considering the dimensionless M-C coefficient C , defined as

$$C \equiv \frac{\tau K}{2\rho c_p d^2} \equiv \frac{\tau \kappa}{2d^2} = \frac{\Gamma}{2}, \quad \text{say,} \quad (2)$$

where ρ is the density, c_p is the specific heat at constant pressure and d is a typical length scale. The factor of two in the definition of C , although standard, leads to redundant powers of two in the subsequent analysis, but with no

* d.w.hughes@leeds.ac.uk

off-setting benefits; we therefore, instead, choose to work in terms of Γ . It is hard to determine the magnitude of Γ in general, but it is typically very small in many astrophysical situations. Does this mean that the effect on, for example, the stability of a convective layer is similarly small? Several remarks are in order here. There is plainly no effect on the threshold for the onset of direct instability, as this occurs when the time derivatives are zero. For ordinary thermal convection, where growth rates are real near onset, the new term has negligible effect for $\Gamma \ll 1$, although oscillatory instability is favoured once Γ becomes $O(10^{-2})$ [9, 10, 13]. Nonetheless, the new term increases the order of the equations describing the linear stability, and so the limit of small Γ is singular; high frequency oscillatory instabilities can then bring the new term into play at very small Γ in certain circumstances, for example in magnetoconvection and double-diffusive convection. These problems have been treated in refs. [34, 35, 38]. In the magnetoconvection problem, in which convection occurs in the presence of an imposed vertical magnetic field, new effects appear when the Chandrasekhar number Q , measuring the square of the imposed field strength, satisfies $Q\Gamma^2 \gtrsim 1$ for small Γ . Similarly, in the double diffusive case, M-C effects become significant, leading to enhanced instability or oscillations, when the gradients of salinity and temperature are both large; specifically, when the salt Rayleigh number Rs is sufficiently large that $Rs\Gamma \gtrsim 1$ for small Γ .

Motivated by these results, in the present paper we consider the other well-known convective instability in the presence of a constraint, namely rotating Rayleigh-Bénard convection. The stability problems for magnetoconvection and rotating convection have a number of similarities but differ in some important details. The classical version of the problem of rotating convection, with applications to planetary and stellar interiors, has a long history, beginning with Chandrasekhar [39, 40] and Veronis [41]. The problem is described by three dimensionless parameters: the Rayleigh number Ra , a measure of the thermal driving; the Taylor number T , proportional to the square of the rotation rate Ω of the layer; and the Prandtl number σ , the ratio of kinematic viscosity to thermal diffusivity — precise definitions of the parameters are given in the following section. In astrophysical and planetary settings, T is typically very large ($T \sim 10^{30}$ in the Earth's outer core, for example) and so here we concentrate on this case of rapid rotation ($T \gg 1$). As we shall show below, M-C effects are significant when $T\Gamma^3 \gtrsim 1$; thus, for $T \gg 1$, M-C effects come into play even for very small values of Γ . We shall also describe how the onset of instability depends in quite a complex manner on σ . A general point of particular note is that, while in the absence of M-C effects ($\Gamma = 0$), oscillatory convection is possible only when the Prandtl number $\sigma < 1$, in the case $\Gamma > 0$ oscillatory instability can be found for a wide range of σ , with a significant reduction in the critical Rayleigh number for the onset of instability.

The mathematical formulation for the linear stability problem is set out in Sec. II. The stability boundary is then investigated separately for the cases $T\Gamma^3 = O(1)$ (Sec. III) and $T\Gamma^3 \gg 1$ (Sec. IV); in each case the scalings for the critical wavenumber, the associated frequency, and the critical Rayleigh number depend strongly on σ when $\sigma \ll 1$, leading to several different scaling regimes. If $\sigma > 1$, on the other hand, the M-C effect permits oscillations that would otherwise not occur. The significance of the results is discussed in the concluding Sec. V.

II. MATHEMATICAL FORMULATION

A. Governing equations

We consider a horizontal layer of an incompressible (Boussinesq) Maxwell-Cattaneo fluid, contained between two planes at $z = 0$ (bottom) and $z = d\pi$ (top), and rotating about the vertical (z) axis with angular velocity Ω . The scaling here with π is helpful in that all factors of π are eliminated from the equations governing the linear stability of the system. The fluid has constant kinematic viscosity ν and thermal diffusivity κ . In the basic state, which is static, the temperature profile is linear in z , with the lower boundary at temperature $T_0 + \Delta T$ and the upper boundary at temperature T_0 . The crucial difference in the governing equations for the M-C system, in comparison with those of classical rotating Boussinesq convection (with no M-C effects) is the replacement of the classical Fourier law by a modified equation for the heat flux; here we adopt the frame-invariant formulation of Christov [37] (see Ref. [38] for further details). On adopting the standard scalings of length with d , time with d^2/κ , temperature with ΔT and pressure with $\rho_0\nu\kappa/d^2$, where ρ_0 is a representative density, the non-dimensional equations governing perturbations from the basic state may be written as

$$\frac{1}{\sigma} \frac{D\mathbf{u}}{Dt} + T^{1/2} \hat{\mathbf{z}} \times \mathbf{u} = -\nabla p + R\theta \hat{\mathbf{z}} + \nabla^2 \mathbf{u}, \quad (3)$$

$$\nabla \cdot \mathbf{u} = 0, \quad (4)$$

$$\frac{D\theta}{Dt} = w - Q, \quad (5)$$

$$\Gamma \frac{DQ}{Dt} = -Q - \nabla^2 \theta. \quad (6)$$

Here $\mathbf{u} = (u, v, w)$ denotes the fluid velocity, θ the perturbation of the temperature from the basic state, Q the divergence of the heat flux and p the pressure. The parameter Γ is as defined in Eq. (2). The Rayleigh number R , Taylor number T , and Prandtl number σ are defined by

$$R = \frac{g\alpha\Delta T d^3}{\kappa\nu}, \quad T = \frac{4\Omega^2 d^4}{\nu^2}, \quad \sigma = \frac{\nu}{\kappa}, \quad (7)$$

where α is the coefficient of thermal expansion.

B. Linearised equations and dispersion relation

In this paper, we address the linear stability of the basic state, subject to the standard boundary conditions in which the horizontal boundaries are impermeable and stress-free, and on which the temperature is fixed. Thus

$$\frac{\partial u}{\partial z} = \frac{\partial v}{\partial z} = w = \theta = 0 \quad \text{on } z = 0, \pi, \quad (8)$$

noting that z is now dimensionless. We assume periodicity in the horizontal directions. In general, we may assume a poloidal-toroidal decomposition for the solenoidal velocity in the form

$$\mathbf{u} = \nabla \times (\nabla \times \mathcal{P} \hat{\mathbf{z}}) + \nabla \times \mathcal{T} \hat{\mathbf{z}}. \quad (9)$$

After linearisation, the z -component of the curl of the momentum equation (3) (the vorticity equation) gives

$$\frac{1}{\sigma} \frac{\partial \mathcal{T}}{\partial t} - T^{1/2} \frac{\partial \mathcal{P}}{\partial z} = \nabla^2 \mathcal{T}. \quad (10)$$

The z -component of a further curl of (3) gives

$$\frac{1}{\sigma} \frac{\partial (\nabla^2 \mathcal{P})}{\partial t} + T^{1/2} \frac{\partial \mathcal{T}}{\partial z} = -R\theta + \nabla^4 \mathcal{P}. \quad (11)$$

The linearised forms of (5) and (6) become, respectively,

$$\frac{\partial \theta}{\partial t} = -\nabla_H^2 \mathcal{P} - Q, \quad (12)$$

$$\Gamma \frac{\partial Q}{\partial t} = -Q - \nabla^2 \theta, \quad (13)$$

where ∇_H^2 is the horizontal Laplacian.

Following the usual approach to the classical rotating convection problem, we seek solutions to the linearised equations of the form

$$\mathcal{P} \propto \theta \propto Q \propto f(x, y) \sin mz e^{st}, \quad \mathcal{T} \propto f(x, y) \cos mz e^{st}, \quad (14)$$

where the planform function $f(x, y)$ satisfies

$$\nabla_H^2 f = -k^2 f. \quad (15)$$

The boundary conditions (8) are thus automatically satisfied. For the classical problem, with no M-C effects, it is easily shown that the fundamental mode (i.e. $m = 1$) is the most readily destabilised. Here we shall also restrict attention to the $m = 1$ mode, but will discuss this assumption in Sec. V, in the light of the results.

Combining equations (10)–(13) gives the following quartic dispersion relation for the growth rate s :

$$a_4 s^4 + a_3 s^3 + a_2 s^2 + a_1 s + a_0 = 0, \quad (16)$$

where

$$a_4 = \Gamma\beta^2, \quad (17a)$$

$$a_3 = (1 + 2\Gamma\sigma\beta^2)\beta^2, \quad (17b)$$

$$a_2 = (1 + 2\sigma)\beta^4 + \Gamma\sigma^2(\beta^6 + T) - \Gamma\sigma Rk^2, \quad (17c)$$

$$a_1 = (2\sigma + \sigma^2)\beta^6 + \sigma^2 T - \sigma Rk^2 - \Gamma\sigma^2 Rk^2\beta^2, \quad (17d)$$

$$a_0 = \sigma^2(\beta^6 + T - Rk^2)\beta^2, \quad (17e)$$

with $\beta^2 = k^2 + 1$. If $\Gamma = 0$, we recover the usual third order system of rotating convection [40].

C. Stability boundaries

The onset of instability may occur either via a steady bifurcation, in which the eigenvalue s passes through zero, or an oscillatory (Hopf) bifurcation, in which $s = \pm i\omega$ ($\omega \in \mathbb{R}_+$). At the onset of steady convection ($s = 0$), the coefficient a_0 , given by (17e), must be zero; thus the value of R is given by

$$R = R^{(s)} = \frac{\beta^6}{k^2} + \frac{T}{k^2}. \quad (18)$$

We shall denote the minimum value of $R^{(s)}$ — the critical value for the onset of steady convection — by $R_c^{(s)}$, and the value of k^2 that gives this minimum — the preferred or favoured mode — by k_{sc}^2 . The criterion for the onset of direct instability (18) is unaffected by any M-C considerations, as is to be expected from the form of the flux equation (6). Thus, any new (i.e. M-C-induced) instability must set in as an oscillatory mode.

At the onset of oscillatory instability, setting $s = i\omega$ in (16) and taking the real and imaginary parts leads to the expressions:

$$a_4\omega^4 - a_2\omega^2 + a_0 = 0, \quad \omega^2 = a_1/a_3. \quad (19)$$

For determining the stability boundary, it is helpful to eliminate ω^2 to obtain the following quadratic expression for R on the oscillatory boundary, which we denote by $R = R^{(o)}$:

$$c_2 \left(R^{(o)} \right)^2 + c_1 R^{(o)} + c_0 = 0, \quad (20)$$

where

$$c_2 = \Gamma^2\sigma^2(1 + \Gamma\sigma\beta^2), \quad (21a)$$

$$c_1 = - \left[2\Gamma^3\sigma^4\frac{\beta^2}{k^2}(\beta^6 + T) + \Gamma^2\sigma^2 \left(2\frac{\beta^6}{k^2} + 3\frac{\sigma}{k^2}(\beta^6 + T) \right) + \Gamma\sigma(1 + 2\sigma)\frac{\beta^4}{k^2} + (1 + \sigma)\frac{\beta^2}{k^2} \right], \quad (21b)$$

$$c_0 = 2\Gamma^2\sigma^4\frac{(\beta^6 + T)^2}{k^4} + 4\Gamma\sigma^2(\sigma - 1)T\frac{\beta^4}{k^4} + 4\Gamma\sigma^2(1 + \sigma)\frac{\beta^{10}}{k^4} + 2\sigma^2T\frac{\beta^2}{k^4} + 2(1 + \sigma)^2\frac{\beta^8}{k^4}. \quad (21c)$$

It is important to note that Eq. (20) defines the oscillatory stability boundary only if the additional condition $\omega^2 > 0$ is satisfied; we denote solutions of (20) with $\omega^2 > 0$ as *admissible* solutions. We shall denote the minimal value of $R^{(o)}$ — the critical value for the onset of oscillatory convection — by $R_c^{(o)}$, the value of k^2 that gives this minimum by k_{oc}^2 , and the corresponding value of ω^2 by ω_c^2 . The overall critical Rayleigh number R_c is then the minimum of $R_c^{(s)}$ and $R_c^{(o)}$.

As we shall see later, to understand whether the steady or oscillatory mode is preferred at the onset of instability, it is helpful to consider the Takens-Bogdanov (T-B) points, defined as those points where the coefficients a_0 and a_1 in (16) are both equal to zero, and which mark the coincidence of the steady and oscillatory stability boundaries. We may regard $a_0 = 0$ and $a_1 = 0$ as two simultaneous equations for Rk^2 , leading to the following quartic equation for β^2 :

$$\Gamma\sigma\beta^8 - (1 + \sigma)\beta^6 + \Gamma\sigma T\beta^2 + (1 - \sigma)T = 0. \quad (22)$$

D. The classical problem

For comparison with later results, it is helpful to recall the conditions for the onset of instability in the classical problem (i.e. no M-C effects). As already noted, $R^{(s)}$, the value of R at the onset of steady convection, is given by expression (18). Here, as discussed in the introduction, we are concerned only with the case of rapid rotation; thus, for $T \gg 1$,

$$R_c^{(s)} \sim 3 \left(\frac{T}{2} \right)^{2/3}, \quad \text{with } k_{sc}^2 \sim \left(\frac{T}{2} \right)^{1/3}. \quad (23)$$

The oscillatory stability boundary is given by

$$R^{(o)} = \frac{2\sigma^2}{1+\sigma} \frac{T}{k^2} + 2(1+\sigma) \frac{\beta^6}{k^2}, \quad (24)$$

provided that

$$\omega^2 = \sigma^2 \left(\left(\frac{1-\sigma}{1+\sigma} \right) \frac{T}{\beta^2} - \beta^4 \right) > 0. \quad (25)$$

Hence, the onset of instability in the classical problem can never be oscillatory if $\sigma > 1$; from (22), there is one T-B point if $\sigma < 1$ and none otherwise.

For $T \gg 1$ (or, more precisely, $\sigma^2 T \gg 1$), the critical value of R for the onset of oscillatory convection is given by

$$R_c^{(o)} \sim 3 \left(\frac{2\sigma^4 T^2}{1+\sigma} \right)^{1/3}, \quad \text{with } k_{oc}^2 \sim \left(\frac{\sigma^2 T}{2(1+\sigma)^2} \right)^{1/3}, \quad \omega_c^2 = \left(\frac{\sigma^2 T}{2(1+\sigma)^2} \right)^{2/3} (2-3\sigma^2), \quad (26)$$

provided $\sigma < \sqrt{2/3} \simeq 0.8164$. From (23) and (26), it can be seen that for $\sigma^2 T \gg 1$, oscillatory convection is preferred for $\sigma < \sigma_c$, where $\sigma_c = 0.6766$ is the (T -independent) positive root of $8\sigma^4 = \sigma + 1$ [40].

For $\sigma^2 T = O(1)$ (with $T \gg 1$, $\sigma \ll 1$), k_{oc}^2 becomes $O(1)$, given by the positive root of the equation (cubic in k_{oc}^2):

$$(2k_{oc}^2 - 1)(1 + 2k_{oc}^2 + k_{oc}^4) = \sigma^2 T. \quad (27)$$

For $\sigma^2 T \ll 1$, $k_{oc}^2 \approx 1/2$, with $R_c^{(o)} \approx 27/2$. In this limit, the critical Rayleigh number becomes independent of T , though we must have $T > 27/8$ to ensure that $\omega^2 > 0$.

For completeness, we note that, even without the assumption of $T \gg 1$, it is possible to find the relationship between T and σ at which there is a transition in the preference for steady or oscillatory modes. Following refs. [42] and [43], one can determine implicit expressions for $R_c^{(s)}$ and $R_c^{(o)}$; equating $R_c^{(s)}$ and $R_c^{(o)}$ then leads to the following expression for T , in terms of σ , denoting when steady and oscillatory modes are equally preferred:

$$T = \frac{27}{2} \frac{(1+\sigma)^{1/2} (\sqrt{2}(1+\sigma)^{1/2} - 1) (1-\sigma)^2 (1+2\sigma)^2}{((1+\sigma)^{1/2} - 2\sqrt{2}\sigma^2)^3}. \quad (28)$$

We may instead regard (28) as an implicit expression for the transitional value of σ , $\sigma_t(T)$; Fig. 1 plots σ_t as a function of T . For $T < T_c = 27(\sqrt{2}-1)/2$, steady convection is always preferred, no matter how small σ . The denominator of expression (28) vanishes when $\sigma = \sigma_c$, where, as introduced above, σ_c is the positive root of $8\sigma^4 = \sigma + 1$; for $\sigma > \sigma_c$, steady convection is always preferred, no matter how large T .

E. When are M-C effects first felt?

The regimes of interest are those in which $T \gg 1$ and $\Gamma \ll 1$. The first point to address therefore is to determine, for a fixed value of $T \gg 1$, how large Γ must be in order that M-C effects are felt. From inspection of the coefficients (21) in the quadratic equation (20) for $R^{(o)}$, it can be seen that with $k_{oc}^2 = O(T^{1/3})$, and assuming that σ is $O(1)$, all of the terms involving Γ in each coefficient are of the same order of magnitude as the Γ -independent terms for $\Gamma = O(T^{-1/3})$. For $\Gamma < O(T^{-1/3})$, the problem is, to leading order, unchanged from the purely hydrodynamic problem. In terms of describing the competition between the influences of rapid rotation and small M-C effect, it is helpful to consider the distinguished limit of $T \gg 1$, $\Gamma = O(T^{-\lambda})$, where $\lambda > 0$ is a dimensionless parameter that allows us to analyse different asymptotic regimes; furthermore, it turns out to be most instructive to consider separately the cases of $\lambda = 1/3$ and $\lambda < 1/3$.

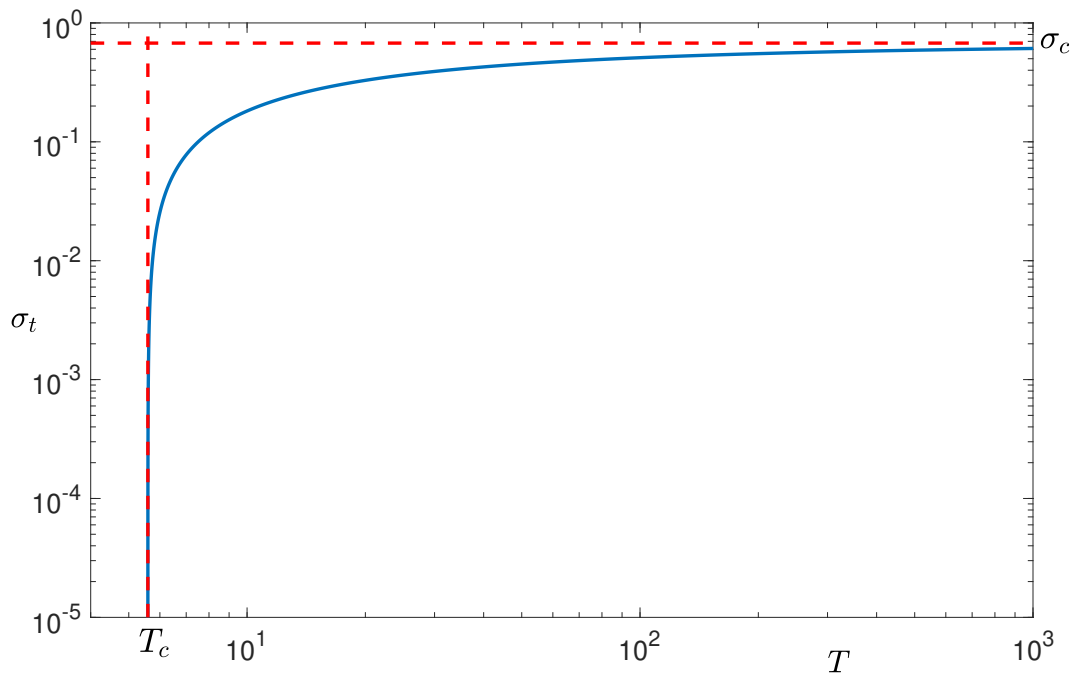


FIG. 1: σ_t , determined by expression (28), as a function of T . Steady (oscillatory) convection is favoured for $\sigma > \sigma_t$ ($\sigma < \sigma_t$). The lines $T = T_c = 27(\sqrt{2} - 1)/2$ and $\sigma = \sigma_c$ (the positive root of $8\sigma^4 = \sigma + 1$) are marked.

III. THE CASE OF $\Gamma = O(T^{-1/3})$

A. General Considerations

For $\Gamma = O(T^{-1/3})$, with $T \gg 1$, the preferred mode for both steady and oscillatory instability has $k^2 = O(T^{1/3})$ (as when $\Gamma = 0$); thus, $\beta^2 \approx k^2$. It is helpful to adopt the scalings

$$T = \Gamma^{-3}\tilde{T}, \quad k^2 = \Gamma^{-1}\tilde{k}^2, \quad R = \Gamma^{-2}\tilde{R}, \quad \omega^2 = \Gamma^{-2}\tilde{\omega}^2. \quad (29)$$

To leading order, the onset of steady convection is therefore given simply by the $T \gg 1$ limit of the classical problem, described by expressions (23). In scaled variables,

$$\tilde{R}_c^{(s)} = 3 \left(\frac{\tilde{T}}{2} \right)^{2/3}, \quad \text{with } \tilde{k}_{sc}^2 = \left(\frac{\tilde{T}}{2} \right)^{1/3}. \quad (30)$$

On substituting the scaled variables (29) into the quadratic equation (20) determining the onset of oscillatory instability, the scaled coefficients of the resulting equation

$$\tilde{c}_2 \left(\tilde{R}^{(o)} \right)^2 + \tilde{c}_1 \tilde{R}^{(o)} + \tilde{c}_0 = 0, \quad (31)$$

become, at leading order,

$$\tilde{c}_2 = \sigma^2(1 + \sigma\tilde{k}^2), \quad (32a)$$

$$\tilde{c}_1 = - \left[2\sigma^4 \left(\tilde{k}^6 + \tilde{T} \right) + \sigma^2 \left((2 + 3\sigma)\tilde{k}^4 + 3\sigma \frac{\tilde{T}}{\tilde{k}^2} \right) + \sigma(1 + 2\sigma)\tilde{k}^2 + (1 + \sigma) \right], \quad (32b)$$

$$\tilde{c}_0 = 2\sigma^4 \frac{(\tilde{k}^6 + \tilde{T})^2}{\tilde{k}^4} + 4\sigma^2(\sigma - 1)\tilde{T} + 4\sigma^2(1 + \sigma)\tilde{k}^6 + \frac{2\sigma^2\tilde{T}}{\tilde{k}^2} + 2(1 + \sigma)^2\tilde{k}^4. \quad (32c)$$

The absence of Γ in the coefficients thus shows the consistency of the scalings (29). In the $\Gamma = O(T^{-1/3})$ regime, both $R_c^{(s)}$ and $R_c^{(o)}$ are thus of the same order, $O(\Gamma^{-2})$; i.e. $\tilde{R}_c^{(s)}$ and $\tilde{R}_c^{(o)}$ are $O(1)$. Determining whether steady or

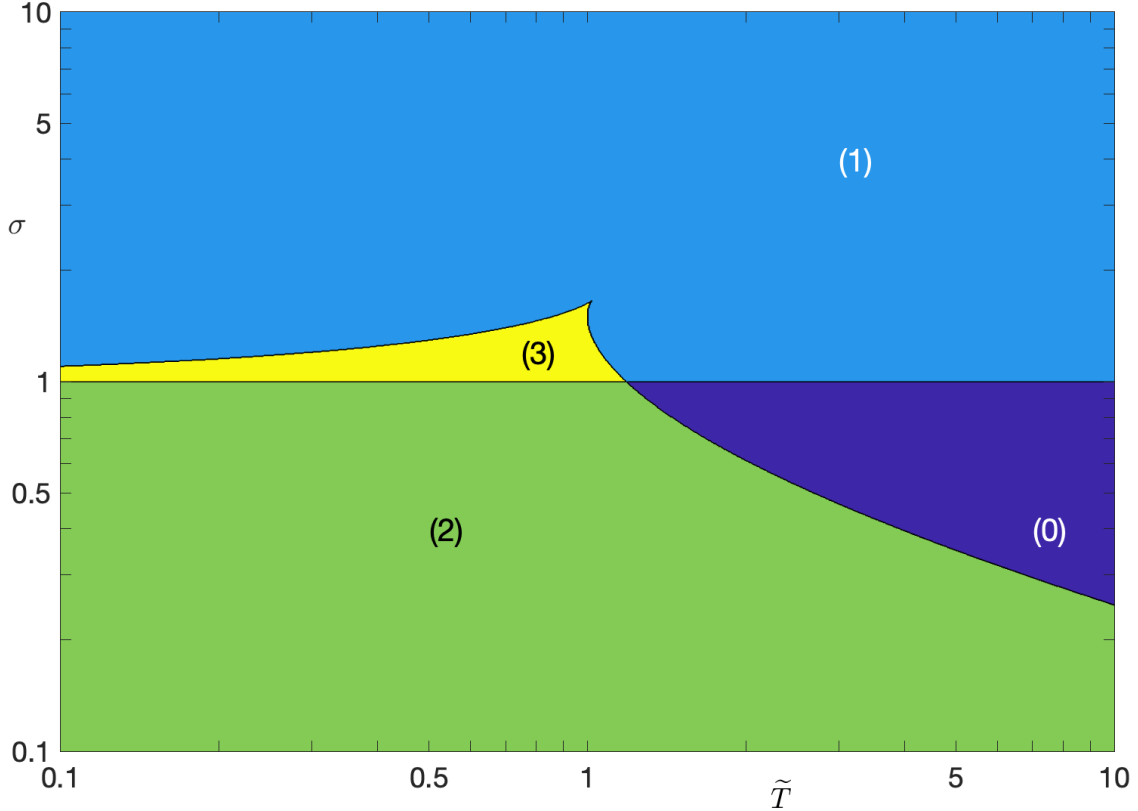


FIG. 2: The number of T-B points, governed by the real positive roots for \tilde{k}^2 of (33), in (\tilde{T}, σ) space.

oscillatory modes are favoured therefore depends on the values of \tilde{T} and σ . Insight into this question can be obtained through consideration of the T-B points. For $\Gamma = O(T^{-1/3})$, with $k^2 \approx \beta^2 = O(T^{1/3}) = O(\Gamma^{-1})$, Eq. (22), which governs the T-B points, becomes, at leading order,

$$\sigma \tilde{k}^8 - (1 + \sigma) \tilde{k}^6 + \sigma \tilde{T} \tilde{k}^2 + (1 - \sigma) \tilde{T} = 0. \quad (33)$$

Figure 2 shows the number of T-B points that are possible as \tilde{T} and σ range over $O(1)$ values. The (\tilde{T}, σ) plane is divided into regions of zero, one, two or three T-B points. The four regions are coincident at $\tilde{T} = 32/27$, $\sigma = 1$; the cusp on the boundary separating the ‘one’ and ‘three’ regions is located at $\tilde{T} = 128/125$, $\sigma = 5/3$. Examples of the stability boundaries for the four regions are illustrated in Fig. 3, which plots the marginal values of \tilde{R} versus \tilde{k}^2 for both steady and oscillatory instability. In Fig. 3(a), there are two T-B points; oscillatory instability is preferred, with $\tilde{k}_{oc}^2 = 0.334$. Figure 3(b) has the same value of σ as in Fig. 3(a), but with an increased value of \tilde{T} ; the two disjoint oscillatory branches in Fig. 3(a) have merged; there are now no T-B points and oscillatory instability is preferred for all wavenumbers. Figure 3(c) illustrates an example with three T-B points. For the case shown, oscillatory instability is preferred, with $\tilde{k}_{oc}^2 = 0.476$; within the zone of three T-B points it is though also possible for the steady mode to be favoured. Figure 3(d) has the same value of \tilde{T} as in Fig. 3(c), but with an increased value of σ . The branch of oscillatory solutions for small \tilde{k}^2 in Fig. 3(c) has collapsed and there is now one T-B point. For the example shown, steady convection is preferred, with $\tilde{k}_{sc}^2 = 0.630$. However, in the large σ regime — with one T-B point — it is also possible for oscillatory convection to be preferred; this is discussed further in §III B.

Although the oscillatory stability boundary is given simply by the quadratic equation (31), for $O(1)$ values of σ , determining the associated critical values of \tilde{R} and \tilde{k}^2 has to be performed numerically. Analytical progress can however be made for the limits of large and small σ .

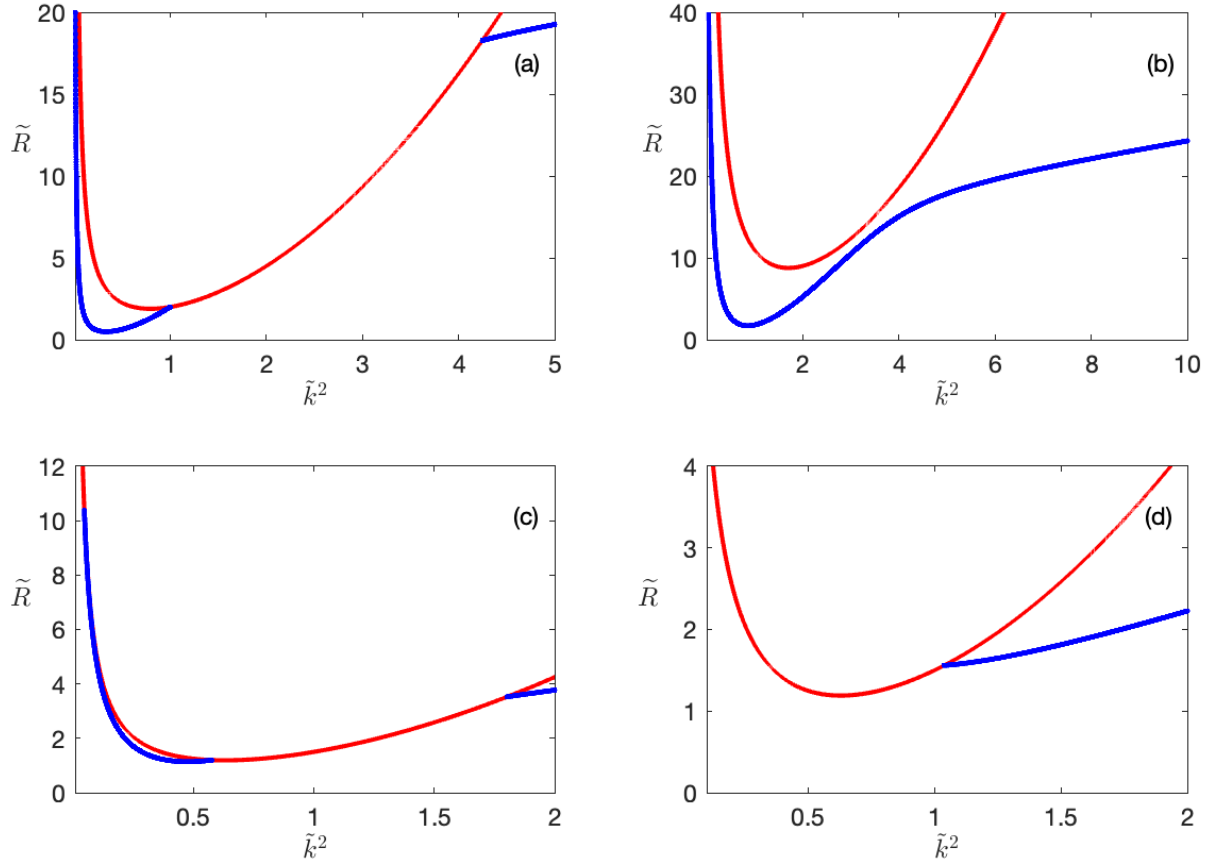


FIG. 3: Examples of marginal stability curves, for \tilde{R} as a function of \tilde{k}^2 , corresponding to the four different regions in Fig. 2; the red lines denote where the steady mode is marginal ($s = 0$), the blue lines where the oscillatory mode is marginal ($s = \pm i\omega$). In (a) (two T-B points), $\tilde{T} = 1$, $\sigma = 0.3$; in (b) (no T-B points), $\tilde{T} = 10$, $\sigma = 0.3$; in (c) (three T-B points), $\tilde{T} = 0.5$, $\sigma = 1.05$; in (d) (one T-B point), $\tilde{T} = 0.5$, $\sigma = 10$.

B. Large σ

The system in Sec. III A, which results from the scaling (29), describes the regime of $T = O(\Gamma^{-3})$, $\Gamma \ll 1$. Here, still within this regime, we consider the case of $\sigma \gg 1$. At leading order in σ , Eq. (31) becomes

$$\tilde{k}^2 \left(\tilde{R}^{(o)} \right)^2 - 2\sigma \left(\tilde{k}^6 + \tilde{T} \right) \tilde{R}^{(o)} + 2\sigma \frac{(\tilde{k}^6 + \tilde{T})^2}{\tilde{k}^4} = 0. \quad (34)$$

The smaller root of (34), which also turns out to be the only admissible solution, is given to leading order by

$$\tilde{R}^{(o)} = \left(\tilde{k}^2 + \frac{\tilde{T}}{\tilde{k}^4} \right). \quad (35)$$

The frequency corresponding to this solution is given, to leading order, by $\tilde{\omega}^2 = \tilde{k}^2 - 1$ and so the solution (35) is admissible provided that $\tilde{k}^2 > 1$. Minimising $\tilde{R}^{(o)}$ over \tilde{k}^2 gives the critical value as

$$\tilde{R}_c^{(o)} = \frac{3}{2} \left(2\tilde{T} \right)^{1/3}, \quad \text{with } \tilde{k}_{oc}^2 \approx \left(2\tilde{T} \right)^{1/3} \quad \text{and } \omega_c^2 \approx \left(2\tilde{T} \right)^{1/3} - 1. \quad (36)$$

The fact that \tilde{k}_{oc}^2 is $O(1)$ underlines the consistency of the approach. Comparison of expressions (30) and (36) shows that steady convection is favoured for $\tilde{T} < 1$, oscillatory convection for $\tilde{T} > 1$. The transition of the preferred mode

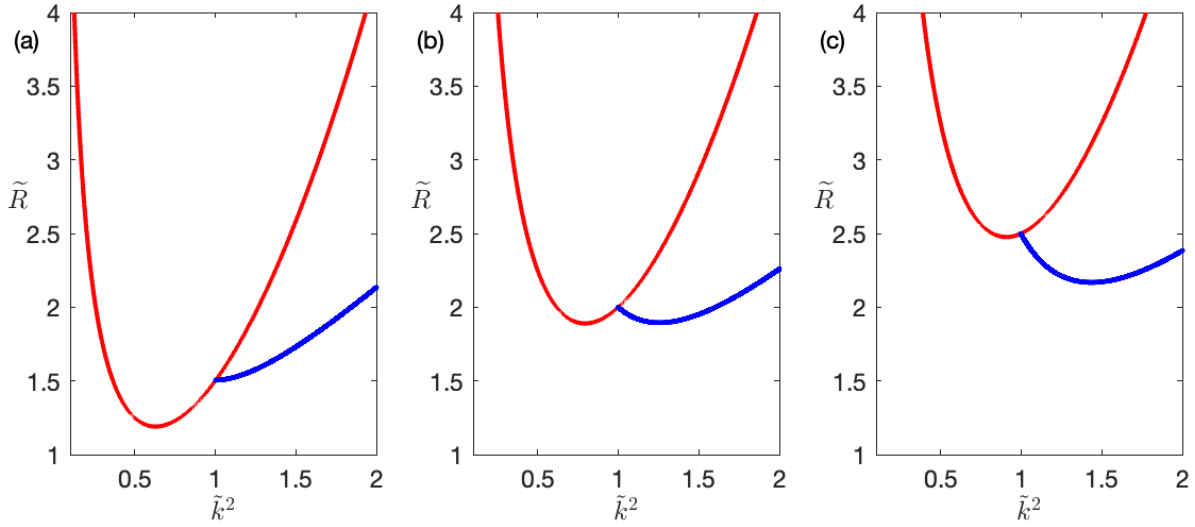


FIG. 4: Marginal stability curves, for \tilde{R} as a function of \tilde{k}^2 with $\sigma = 10^2$; the red and blue lines denote, respectively, where the steady and oscillatory modes are marginal. In (a), $\tilde{T} = 0.5$; in (b), $\tilde{T} = 1$; in (c), $\tilde{T} = 1.5$.

as \tilde{T} is changed is illustrated in Fig. 4, which shows the plots of the stability boundaries for \tilde{R} as a function of \tilde{k}^2 for $\sigma = 10^2$. In Fig. 4(a), $\tilde{T} = 0.5$ and steady convection is preferred (this is also the regime shown in Fig. 3(d)); in Fig. 4(b), $\tilde{T} = 1$ and the minima of \tilde{R} for the steady and oscillatory modes are the same, with different associated values of \tilde{k}^2 ; in Fig. 4(c), $\tilde{T} = 1.5$ and oscillatory convection is preferred. The difference between the case of $\Gamma = O(T^{-1/3})$ and the classical case of $\Gamma = 0$ is noteworthy: with the M-C effect, oscillatory convection can be preferred even for $\sigma \gg 1$ (as in Fig. 4(c)), whereas for the classical problem, the oscillatory branch does not even exist for $\sigma > 1$.

C. Small σ

A naive small σ limit of (31), keeping \tilde{k}^2 to be $O(1)$, gives $\tilde{R}^{(o)} \approx 2\tilde{k}^4$. Since, from this approximation, $\tilde{R}^{(o)}$ is minimised at $\tilde{k}^2 = 0$, it follows that we must consider asymptotically smaller values of \tilde{k}^2 in order to capture the true minimum. Hence, as σ is decreased from $O(1)$ values, \tilde{k}^2 must also be reduced; the reduction must be such that, for the coefficients (32), terms with \tilde{k}^2 in the denominator are brought into play. This first occurs when the penultimate term in (32c) becomes large enough to balance the ultimate term, implying that $\tilde{k}^2 = O(\sigma^{2/3})$, with both these terms $O(\sigma^{4/3})$. We thus adopt the further rescalings of $\tilde{k}^2 = \sigma^{2/3}\hat{k}^2$, $\tilde{\omega}^2 = \sigma^{4/3}\hat{\omega}^2$, which give, at leading order in σ ,

$$\tilde{R}^{(o)} = 2\sigma^{4/3} \left(\hat{k}^4 + \frac{\tilde{T}}{\hat{k}^2} \right). \quad (37)$$

Expression (37) results from terms in the coefficients (32) (or, more explicitly, (21)) that do not involve Γ ; thus, at this level of approximation, we simply recover the expression for the onset of oscillatory convection in the classical problem for large T , small σ . As anticipated, the minimum of $\tilde{R}^{(o)}$ is thus captured for $O(1)$ values of \hat{k}^2 ; it is given by

$$\tilde{R}_c^{(o)} = 6 \left(\frac{\sigma^2 \tilde{T}}{2} \right)^{2/3}, \quad \text{with} \quad \hat{k}_{oc}^2 = \left(\frac{\tilde{T}}{2} \right)^{1/3} \quad \text{and} \quad \hat{\omega}_c^2 = \left(2\tilde{T}^2 \right)^{1/3}. \quad (38)$$

Equivalently, on reverting to the unscaled variables, this becomes

$$R_c^{(o)} = 6 \left(\frac{\sigma^2 T}{2} \right)^{2/3}, \quad \text{with} \quad k_{oc}^2 = \left(\frac{\sigma^2 T}{2} \right)^{1/3} \quad \text{and} \quad \omega_c^2 = (2\sigma^4 T^2)^{1/3}. \quad (39)$$

We note that since $\tilde{R}_c^{(o)}$ scales with $\sigma^{4/3}$, where σ is assumed small, then it is formally smaller than $\tilde{R}_c^{(s)}$, which is $O(1)$ and independent of σ ; thus, for small σ , oscillatory convection is always preferred. Numerical solution shows that expression (38) provides a better approximation for \tilde{k}_{oc}^2 than it does for $\tilde{R}_c^{(o)}$ (although they are both correct to leading order). It turns out, however, that the next-order correction to $\tilde{R}_c^{(o)}$ is independent of \hat{k}^2 , and so we can improve our estimate for $\tilde{R}_c^{(o)}$ without having to calculate the next-order correction to \hat{k}_{oc}^2 ; this gives

$$\tilde{R}_c^{(o)} = 6 \left(\frac{\sigma^2 \tilde{T}}{2} \right)^{2/3} - 4\sigma^2 \tilde{T}, \quad (40)$$

or, in terms of the unscaled variables,

$$R_c^{(o)} = 6 \left(\frac{\sigma^2 T}{2} \right)^{2/3} - 4\sigma^2 \Gamma T. \quad (41)$$

The correction term in (41), which depends on Γ , is asymptotically large compared with the next-order correction to the classical problem, which is $O(\sigma^{7/3} T^{2/3})$. Table I contains the values of \tilde{k}_{oc}^2 , ω_c^2 and $R_c^{(o)}$ calculated from the full system, for three values of σ , with $\Gamma = 10^{-6}$ and $T = 10^{18}$, together with the small σ asymptotic results (39) and (41). It can be seen that the approximation (39) for \tilde{k}_{oc}^2 is indeed much more accurate than the corresponding expression for $\tilde{R}_c^{(o)}$; the improvement in the estimate (40) for $R_c^{(o)}$ is also evident.

TABLE I: Values of \tilde{k}_{oc}^2 , ω_c^2 and $R_c^{(o)}$ calculated from the full system and from the asymptotic expressions (39) and (41), for three values of σ , with $\Gamma = 10^{-6}$ and $T = 10^{18}$, together with $R_c^{(o)}$ from the classical ($\Gamma = 0$) problem with $T = 10^{18}$.

σ	\tilde{k}_{oc}^2 (full)	ω_c^2 (full)	$R_c^{(o)}$ (full)	\tilde{k}_{oc}^2 (Eq. (39))	ω_c^2 (Eq. (39))	$R_c^{(o)}$ (Eq. (39))	$R_c^{(o)}$ (Eq. (40))	$R_c^{(o)}$ (classical)
10^{-1}	1.6656×10^5	5.0014×10^{10}	1.3952×10^{11}	1.7100×10^5	5.8480×10^{10}	1.7544×10^{11}	1.3544×10^{11}	1.6996×10^{11}
10^{-2}	3.6668×10^4	2.6748×10^9	7.7357×10^9	3.6840×10^4	2.7144×10^9	8.1433×10^9	7.7433×10^9	8.1165×10^9
10^{-3}	7.9319×10^3	1.2581×10^8	3.7393×10^8	7.9370×10^3	1.2599×10^8	3.7798×10^8	3.7398×10^8	3.7790×10^8

The scaling of \tilde{k}_{oc}^2 with $\sigma^{2/3}$ persists with decreasing σ until \tilde{k}_{oc}^2 becomes sufficiently small that the approximation $\beta^2 = k^2$ fails; i.e. when $\tilde{k}_{oc}^2 = O(1)$ or, equivalently, when $\tilde{k}_{oc}^2 = O(\Gamma)$. Thus expression (39), and its improvement (41), holds for the entire range $O(1) > \sigma > O(\Gamma^{3/2})$.

For $\sigma = O(\Gamma^{3/2})$ (i.e. $\sigma^2 T = O(1)$), we must revert to the full system, where β^2 is no longer approximated by k^2 . From (20), with coefficients (21), we then obtain, at leading order,

$$R^{(o)} = 2 \left(\frac{\beta^6}{k^2} + \frac{\sigma^2 T}{k^2} \right). \quad (42)$$

We have thus just recovered (24), the expression for oscillatory onset in the classical problem for $\sigma^2 T = O(1)$. For yet smaller σ , with $\sigma^2 T \ll 1$, we are left with only the first term in (42); as discussed earlier, this gives $\tilde{k}_{oc}^2 = 1/2$, $\omega_c^2 = (8T - 27)\sigma^2/12$, $R_c^{(o)} = 27/2$.

IV. THE CASE OF $\Gamma > O(T^{-1/3})$

We now consider the case of $\Gamma = O(T^{-\lambda})$, with $\lambda < 1/3$. As we shall describe below, the wavenumber of the mode of maximum growth rate, the associated frequency, and the critical Rayleigh number depend crucially on the Prandtl number σ . A number of distinct asymptotic regimes can be identified, covering the entire range of σ ; we investigate these separately in the following subsections, tying the results together, for the entire range of σ , in Sec. IV C.

A. $\sigma \gtrsim O(1)$

For $\sigma \gtrsim O(1)$, the preferred mode for oscillatory instability has $k^2 = O(\Gamma^{-1/3\lambda})$; thus, again, $\beta^2 \approx k^2$. Under this scaling, the coefficients of the quadratic equation (20) determining $R^{(o)}$ are, to leading order in Γ ,

$$c_2 = \Gamma^3 \sigma^3 k^2 = O(\Gamma^{3-1/3\lambda}), \quad (43a)$$

$$c_1 = -2\Gamma^3 \sigma^4 (k^6 + T) = O(\Gamma^{3-1/\lambda}), \quad (43b)$$

$$c_0 = 2\Gamma^2 \sigma^4 \frac{(k^6 + T)^2}{k^4} = O(\Gamma^{2-4/3\lambda}). \quad (43c)$$

The relative sizes of the coefficients imply that the two roots for $R^{(o)}$ are $O(\Gamma^{-1-1/3\lambda})$ and $O(\Gamma^{-2/3\lambda})$. It is straightforward to show that only the former (smaller) root is admissible. On adopting the scalings

$$T = \Gamma^{-1/\lambda} \tilde{T}, \quad k^2 = \Gamma^{-1/3\lambda} \tilde{k}^2, \quad \omega^2 = \Gamma^{-1-1/3\lambda} \tilde{\omega}^2, \quad R = \Gamma^{-1-1/3\lambda} \tilde{R}, \quad (44)$$

we obtain

$$\tilde{R}^{(o)} = \tilde{k}^2 + \frac{\tilde{T}}{\tilde{k}^4}; \quad (45)$$

the minimum value of $\tilde{R}^{(o)}$ is given by

$$\tilde{R}_c^{(o)} = 3 \left(\frac{\tilde{T}}{4} \right)^{1/3}, \quad \text{with} \quad \tilde{k}_{oc}^2 = (2\tilde{T})^{1/3} \quad \text{and} \quad \tilde{\omega}_c^2 = (2\tilde{T})^{1/3}. \quad (46)$$

In unscaled variables, these expressions become

$$R_c^{(o)} = 3\Gamma^{-1} \left(\frac{T}{4} \right)^{1/3}, \quad \text{with} \quad k_{oc}^2 = (2T)^{1/3} \quad \text{and} \quad \omega_c^2 = \Gamma^{-1} (2T)^{1/3}. \quad (47)$$

Recalling that the onset of steady convection for $T \gg 1$ is always given by (23), gives $R_c^{(s)} = O(T^{2/3}) = O(\Gamma^{-2/3\lambda})$. Since $R_c^{(o)} = O(\Gamma^{-1-1/3\lambda})$, $R_c^{(s)}$ is formally asymptotically larger than $R_c^{(o)}$ for $\lambda < 1/3$. Hence, in this regime, we need restrict attention only to the onset of oscillatory convection, since this is always preferred.

TABLE II: Values of k_{oc}^2 , ω_c^2 and $R_c^{(o)}$ for the full system for five values of σ , with $\Gamma = 10^{-4}$ and $T = 10^{16}$ ($\lambda = 1/4$), together with the σ -independent asymptotic expressions (47).

σ	k_{oc}^2 (full)	ω_c^2 (full)	$R_c^{(o)}$ (full)	k_{oc}^2 (Eq. (47))	ω_c^2 (Eq. (47))	$R_c^{(o)}$ (Eq. (47))
100	2.7139×10^5	2.6136×10^9	4.0721×10^9	2.7144×10^5	2.7144×10^9	4.0716×10^9
10	2.7085×10^5	2.6052×10^9	4.0763×10^9	2.7144×10^5	2.7144×10^9	4.0716×10^9
1	2.5778×10^5	2.4498×10^9	4.0851×10^9	2.7144×10^5	2.7144×10^9	4.0716×10^9
0.5	2.3004×10^5	2.1659×10^9	4.0034×10^9	2.7144×10^5	2.7144×10^9	4.0716×10^9
0.1	0.9094×10^5	0.8772×10^9	1.9043×10^9	2.7144×10^5	2.7144×10^9	4.0716×10^9

Table II contains the values of k_{oc}^2 , ω_c^2 and $R_c^{(o)}$ calculated numerically from the full system, for five values of σ , with $\Gamma = 10^{-4}$ and $T = 10^{16}$ ($\lambda = 1/4$), together with the σ -independent asymptotic results (47); the asymptotic expression for ω_c^2 , given by (47), is not in such good agreement as those for k_{oc}^2 and $R_c^{(o)}$, since the next order correction is formally larger. It can be seen that the agreement between the full and approximate results is very good for $\sigma \geq 1$, but that for $\sigma < 1$, expressions (47) cease to be accurate. Indeed, by $\sigma = 0.1$, which is not a particularly small value of σ , there is no resemblance between the two sets of results. It is clear, therefore, that for $\sigma < 1$, the dominant balance in Eq. (20) will no longer be provided by the coefficients (43). As described in the following subsection, the picture for small σ is quite intricate.

B. Small σ

As σ is reduced below unity, the dominant balance of the coefficients ceases to be represented by equations (43), which yield expressions for k_{oc}^2 and $R_c^{(o)}$ that are independent of σ . As described below, there are two broad asymptotic regimes to consider, determined by the size of σ .

$$1. \quad O\left(\Gamma^{(1-3\lambda)/2\lambda}\right) \lesssim \sigma \lesssim O\left(\Gamma^{(1-3\lambda)/6\lambda}\right)$$

With the scaling $k^2 = O(\Gamma^{-1/3\lambda})$, valid for $\sigma = O(1)$, expressions (43) first cease to be accurate when $\sigma = O(\Gamma^{(1-3\lambda)/6\lambda})$. To leading order, the coefficients (21) then become

$$c_2 = \Gamma^3 \sigma^3 k^2 = O\left(\Gamma^{(1+9\lambda)/6\lambda}\right), \quad (48a)$$

$$c_1 = -2\left(\Gamma^3 \sigma^4 (k^6 + T) + \Gamma^2 \sigma^2 k^4\right) = O\left(\Gamma^{1-1/3\lambda}\right), \quad (48b)$$

$$c_0 = 2\Gamma^2 \sigma^4 \frac{(k^6 + T)^2}{k^4} - 4\Gamma \sigma^2 T + 4\Gamma \sigma^2 k^6 + 2k^4 = O\left(\Gamma^{-2/3\lambda}\right). \quad (48c)$$

Thus, to leading order, R is determined by $R = -c_0/c_1$. On writing

$$T = \Gamma^{-1/\lambda} \tilde{T}, \quad \sigma = \Gamma^{(1-3\lambda)/6\lambda} \tilde{\sigma}, \quad k^2 = \Gamma^{-1/3\lambda} \tilde{k}^2, \quad \omega^2 = \Gamma^{-(1+3\lambda)/3\lambda} \tilde{\omega}^2, \quad R = \Gamma^{-(1+3\lambda)/3\lambda} \tilde{R}, \quad (49)$$

we obtain

$$\tilde{R} = \frac{\tilde{\sigma}^4 \left(\tilde{k}^6 + \tilde{T}\right)^2 - 2\tilde{\sigma}^2 \tilde{T} \tilde{k}^4 + 2\tilde{\sigma}^2 \tilde{k}^{10} + \tilde{k}^8}{\tilde{\sigma}^4 \left(\tilde{k}^6 + \tilde{T}\right) \tilde{k}^4 + \tilde{\sigma}^2 \tilde{k}^8}. \quad (50)$$

Expression (45) is recovered through the large $\tilde{\sigma}$ limit of (50). The stationary points for \tilde{R} (i.e. where $d\tilde{R}/d\tilde{k}^2 = 0$) are given by the roots of the following ninth order polynomial for \tilde{k}^2 :

$$\tilde{\sigma}^4 \tilde{k}^{18} + 2\tilde{\sigma}^2 \tilde{k}^{16} + \tilde{k}^{14} + 10\tilde{\sigma}^2 \tilde{T} \tilde{k}^{10} + 6\tilde{T} \tilde{k}^8 - 3\tilde{\sigma}^4 \tilde{T}^2 \tilde{k}^6 - 4\tilde{\sigma}^2 \tilde{T}^2 \tilde{k}^4 - 2\tilde{\sigma}^4 \tilde{T}^3 = 0. \quad (51)$$

The frequency is given by the simple relation

$$\tilde{\omega}^2 = \tilde{k}^2. \quad (52)$$

Equation (51) has no obvious factorisation; numerical solutions for $O(1)$ values of $\tilde{\sigma}$ and \tilde{T} suggest that there is just one minimum of \tilde{R} for $\tilde{k}^2 > 0$. For the representative case of $\tilde{T} = 1$ and $\tilde{\sigma} = 1$, the critical value of \tilde{k}^2 is given, from solution of (51), by $\tilde{k}_{oc}^2 = 0.7879$, with $\omega_c^2 = 0.7879$ and $\tilde{R}_c^{(o)} = 1.5029$, from (52) and (50) respectively. Table III contains the values of k_{oc}^2 , ω_c^2 and $R_c^{(o)}$ calculated from the full system, with $\tilde{T} = \tilde{\sigma} = 1$ and for a range of values of Γ and λ , and compares them with the respective results obtained from (51), (52) and (50), together with the scaling (49). As expected, the agreement improves as either Γ or λ is decreased.

As $\tilde{\sigma}$ decreases, so does \tilde{k}^2 . Thus, for small $\tilde{\sigma}$, retaining the leading order terms in expression (51) gives the simpler expression,

$$6\tilde{T} \tilde{k}^8 - 4\tilde{\sigma}^2 \tilde{T}^2 \tilde{k}^4 - 2\tilde{\sigma}^4 \tilde{T}^3 = 0, \quad (53)$$

which factorises to give the one admissible solution,

$$\tilde{k}^2 = \tilde{k}_{oc}^2 = \tilde{\sigma} \tilde{T}^{1/2} \implies k_{oc}^2 = \sigma \sqrt{\Gamma T}. \quad (54)$$

From (52), we thus have

$$\omega_c^2 = \sigma \sqrt{T/\Gamma}. \quad (55)$$

TABLE III: Values of k_{oc}^2 , ω_c^2 and $R_c^{(o)}$ for the full system and from the respective asymptotic expressions (51), (52) and (50), rescaled by (49), for $\tilde{T} = \tilde{\sigma} = 1$ and for three values of both λ and Γ .

λ	Γ	T	σ	k_{oc}^2 (full)	ω_c^2 (full)	$R_c^{(o)}$ (full)	k_{oc}^2 (Eq. (51))	ω_c^2 (Eq. (52))	$R_c^{(o)}$ (Eq. (50))
1/4	10 ⁻⁴	10 ¹⁶	10 ^{-2/3}	1.5785 × 10 ⁵	1.5019 × 10 ⁹	3.2868 × 10 ⁹	1.6974 × 10 ⁵	1.6974 × 10 ⁹	3.2380 × 10 ⁹
1/4	10 ⁻⁵	10 ²⁰	10 ^{-5/6}	3.4765 × 10 ⁶	3.388 × 10 ¹¹	7.0515 × 10 ¹¹	3.6570 × 10 ⁶	3.6570 × 10 ¹¹	6.9760 × 10 ¹¹
1/4	10 ⁻⁶	10 ²⁴	10 ⁻¹	7.6078 × 10 ⁷	7.5023 × 10 ¹³	1.5144 × 10 ¹⁴	7.8787 × 10 ⁷	7.8787 × 10 ¹³	1.5029 × 10 ¹⁴
1/5	10 ⁻⁴	10 ²⁰	10 ^{-4/3}	3.5971 × 10 ⁶	3.5805 × 10 ¹⁰	7.0015 × 10 ¹⁰	3.6570 × 10 ⁶	3.6570 × 10 ¹⁰	6.9760 × 10 ¹⁰
1/5	10 ⁻⁵	10 ²⁵	10 ^{-5/3}	1.6844 × 10 ⁸	1.6814 × 10 ¹³	3.2436 × 10 ¹³	1.6974 × 10 ⁸	1.6974 × 10 ¹³	3.2380 × 10 ¹³
1/5	10 ⁻⁶	10 ³⁰	10 ⁻²	7.8505 × 10 ⁹	7.8447 × 10 ¹⁵	1.5041 × 10 ¹⁶	7.8787 × 10 ⁹	7.8787 × 10 ¹⁵	1.5029 × 10 ¹⁶
1/6	10 ⁻⁴	10 ²⁴	10 ⁻²	7.8505 × 10 ⁷	7.8447 × 10 ¹¹	1.5041 × 10 ¹²	7.8787 × 10 ⁷	7.8787 × 10 ¹¹	1.5029 × 10 ¹²
1/6	10 ⁻⁵	10 ³⁰	10 ^{-5/2}	7.8698 × 10 ⁹	7.8681 × 10 ¹⁴	1.5033 × 10 ¹⁵	7.8787 × 10 ⁹	7.8787 × 10 ¹⁴	1.5029 × 10 ¹⁵
1/6	10 ⁻⁶	10 ³⁶	10 ⁻³	7.8759 × 10 ¹¹	7.8754 × 10 ¹⁷	1.5031 × 10 ¹⁸	7.8787 × 10 ¹¹	7.8787 × 10 ¹⁷	1.5029 × 10 ¹⁸

To determine $\tilde{R}_c^{(o)}$, it is helpful to rewrite expression (50) as

$$\tilde{R} = \frac{\left(\tilde{k}^4 - \tilde{\sigma}^2 \tilde{T}\right)^2 + 2\tilde{\sigma}^4 \tilde{T} \tilde{k}^6 + 2\tilde{\sigma}^2 \tilde{k}^{10} + \tilde{\sigma}^4 \tilde{k}^{12}}{\tilde{\sigma}^4 \tilde{T} \tilde{k}^4 + \tilde{\sigma}^2 \tilde{k}^8 + \tilde{\sigma}^4 \tilde{k}^{10}}. \quad (56)$$

With $\tilde{k}^2 = \tilde{T}^{1/2} \tilde{\sigma}$, the leading order terms in \tilde{R} (i.e. terms of $O(\tilde{\sigma}^4)$) cancel, giving $\tilde{R}_c^{(o)} = 0$ at this order. The perfect square in the numerator in (56) does though enable us to evaluate the leading-order finite contribution to $\tilde{R}_c^{(o)}$ without needing the next-order correction to \tilde{k}_{oc}^2 . Indeed, we obtain the surprisingly simple expression,

$$\tilde{R}_c^{(o)} = 2\tilde{\sigma} \tilde{T}^{1/2} \implies R_c^{(o)} = 2\sigma \sqrt{\frac{T}{\Gamma}} = \frac{2k_c^2}{\Gamma}. \quad (57)$$

Table IV contains the values of k_{oc}^2 , ω_c^2 and $R_c^{(o)}$ calculated from the full system, with $\tilde{T} = 1$ and $\tilde{\sigma} = 0.1$, for a range of values of Γ and λ , and compares them with the respective asymptotic results (54), (55) and (57). The agreement is particularly good for the smaller values of Γ and λ .

TABLE IV: Values of k_{oc}^2 , ω_c^2 and $R_c^{(o)}$ for the full system and from the asymptotic expressions (54), (55) and (57), for $\tilde{T} = 1$, $\tilde{\sigma} = 0.1$ and for three values of both λ and Γ .

λ	Γ	T	σ	k_{oc}^2 (full)	ω_c^2 (full)	$R_c^{(o)}$ (full)	$\sigma\sqrt{\Gamma T}$ (Eq. (54))	$\sigma\sqrt{T/\Gamma}$ (Eq. (55))	$2\sigma\sqrt{T/\Gamma}$ (Eq. (57))
1/4	10 ⁻⁴	10 ¹⁶	10 ^{-5/3}	2.2394 × 10 ⁴	2.0032 × 10 ⁸	4.1871 × 10 ⁸	2.1544 × 10 ⁴	2.1544 × 10 ⁸	4.3089 × 10 ⁸
1/4	10 ⁻⁵	10 ²⁰	10 ^{-11/6}	4.7114 × 10 ⁵	4.4677 × 10 ¹⁰	9.1558 × 10 ¹⁰	4.6416 × 10 ⁵	4.6416 × 10 ¹⁰	9.2832 × 10 ¹⁰
1/4	10 ⁻⁶	10 ²⁴	10 ⁻²	1.0044 × 10 ⁷	0.9797 × 10 ¹³	1.9866 × 10 ¹³	1 × 10 ⁷	1 × 10 ¹³	2 × 10 ¹³
1/5	10 ⁻⁴	10 ²⁰	10 ^{-7/3}	4.6356 × 10 ⁵	4.6107 × 10 ⁹	9.2661 × 10 ⁹	4.6416 × 10 ⁵	4.6416 × 10 ⁹	9.2832 × 10 ⁹
1/5	10 ⁻⁵	10 ²⁵	10 ^{-8/3}	2.1511 × 10 ⁷	2.1486 × 10 ¹²	4.3055 × 10 ¹²	2.1544 × 10 ⁷	2.1544 × 10 ¹²	4.3089 × 10 ¹²
1/5	10 ⁻⁶	10 ³⁰	10 ⁻³	9.9888 × 10 ⁸	9.9863 × 10 ¹⁴	1.9989 × 10 ¹⁵	1 × 10 ⁹	1 × 10 ¹⁵	2 × 10 ¹⁵
1/6	10 ⁻⁴	10 ²⁴	10 ⁻³	9.9888 × 10 ⁶	9.9863 × 10 ¹⁰	1.9989 × 10 ¹¹	1 × 10 ⁷	1 × 10 ¹¹	2 × 10 ¹¹
1/6	10 ⁻⁵	10 ³⁰	10 ^{-7/2}	9.9928 × 10 ⁸	9.9925 × 10 ¹³	1.9990 × 10 ¹⁴	1 × 10 ⁹	1 × 10 ¹⁴	2 × 10 ¹⁴
1/6	10 ⁻⁶	10 ³⁶	10 ⁻⁴	9.9943 × 10 ¹⁰	9.9942 × 10 ¹⁶	1.9990 × 10 ¹⁷	1 × 10 ¹¹	1 × 10 ¹⁷	2 × 10 ¹⁷

$$2. \quad \sigma \lesssim O\left(\Gamma^{(1-3\lambda)/2\lambda}\right)$$

There is a further change in the dominant balance of the coefficients of Eq. (20) when $\sigma = O(\Gamma^{(1-3\lambda)/2\lambda})$, $k^2 = O(\Gamma^{-1})$. The coefficient c_1 can then be approximated by $c_1 = -1$, giving, to leading order,

$$R^{(o)} = \frac{2\Gamma^2 \sigma^4 T^2}{k^4} - 4\Gamma T \sigma^2 + \frac{2\sigma^2 T}{k^2} + 2k^4. \quad (58)$$

On writing

$$T = \Gamma^{-1/\lambda} \tilde{T}, \quad \sigma = \Gamma^{(1-3\lambda)/2\lambda} \tilde{\sigma}, \quad k^2 = \Gamma^{-1} \tilde{k}^2, \quad \omega^2 = \Gamma^{-2} \tilde{\omega}^2, \quad R^{(o)} = \Gamma^{-2} \tilde{R}^{(o)}, \quad (59)$$

we obtain

$$\tilde{R}^{(o)} = \frac{2\tilde{\sigma}^4 \tilde{T}^2}{\tilde{k}^4} - 4\tilde{T} \tilde{\sigma}^2 + \frac{2\tilde{\sigma}^2 \tilde{T}}{\tilde{k}^2} + 2\tilde{k}^4, \quad (60)$$

with $\tilde{R}^{(o)}$ minimised when

$$2\tilde{k}^8 - \tilde{\sigma}^2 \tilde{T} \tilde{k}^2 - 2\tilde{\sigma}^4 \tilde{T}^2 = 0. \quad (61)$$

The frequency is then given by

$$\tilde{\omega}^2 = \frac{\tilde{\sigma}^2 \tilde{T}}{\tilde{k}^2}. \quad (62)$$

The large $\tilde{\sigma}$ limit of (61) gives $\tilde{k}^2 = \tilde{k}_{oc}^2 \approx \tilde{\sigma} \sqrt{\tilde{T}}$; in dimensional units, this translates to $k_{oc}^2 = \sigma \sqrt{\Gamma T}$, thus recovering expression (54). Table V contains the values of k_{oc}^2 , ω_c^2 and $R_c^{(o)}$ calculated from the full system, with $\tilde{T} = 1$ and $\tilde{\sigma} = 1$ (with $\tilde{\sigma}$ defined by (59)), for a range of values of Γ and λ , and compares them with the respective asymptotic results (61), (62) and (60), rescaled via (59). Once again, the agreement is particularly good for the smaller values of Γ and λ .

TABLE V: Values of k_{oc}^2 , ω_c^2 and $R_c^{(o)}$ for the full system and from the respective asymptotic expressions (61), (62) and (60), rescaled by (59), for $\tilde{T} = 1$, $\tilde{\sigma} = 1$ and for three values of both λ and Γ .

λ	Γ	T	σ	k_{oc}^2 (full)	ω_c^2 (full)	$R_c^{(o)}$ (full)	k_{oc}^2 (Eq. (61))	ω_c^2 (Eq. (62))	$R_c^{(o)}$ (Eq. (60))
1/4	10 ⁻⁴	10 ¹⁶	10 ⁻²	1.1093 × 10 ⁴	8.8734 × 10 ⁷	1.8882 × 10 ⁸	1.1173 × 10 ⁴	8.9498 × 10 ⁷	1.8889 × 10 ⁸
1/4	10 ⁻⁵	10 ²⁰	10 ^{-5/2}	1.1148 × 10 ⁵	8.9258 × 10 ⁹	1.8886 × 10 ¹⁰	1.1173 × 10 ⁵	8.9498 × 10 ⁹	1.8889 × 10 ¹⁰
1/4	10 ⁻⁶	10 ²⁴	10 ⁻³	1.1166 × 10 ⁶	8.9422 × 10 ¹¹	1.8888 × 10 ¹²	1.1173 × 10 ⁶	8.9498 × 10 ¹¹	1.8889 × 10 ¹²
1/5	10 ⁻⁴	10 ²⁰	10 ⁻⁴	1.1172 × 10 ⁴	8.9489 × 10 ⁷	1.8890 × 10 ⁸	1.1173 × 10 ⁴	8.9498 × 10 ⁷	1.8889 × 10 ⁸
1/5	10 ⁻⁵	10 ²⁵	10 ⁻⁵	1.1173 × 10 ⁵	8.9497 × 10 ⁹	1.8889 × 10 ¹⁰	1.1173 × 10 ⁵	8.9498 × 10 ⁹	1.8889 × 10 ¹⁰
1/5	10 ⁻⁶	10 ³⁰	10 ⁻⁶	1.1173 × 10 ⁶	8.9497 × 10 ¹¹	1.8889 × 10 ¹²	1.1173 × 10 ⁶	8.9498 × 10 ¹¹	1.8889 × 10 ¹²
1/6	10 ⁻⁴	10 ²⁴	10 ⁻⁶	1.1173 × 10 ⁴	8.9497 × 10 ⁷	1.8890 × 10 ⁸	1.1173 × 10 ⁴	8.9498 × 10 ⁷	1.8889 × 10 ⁸
1/6	10 ⁻⁵	10 ³⁰	10 ^{-15/2}	1.1173 × 10 ⁵	8.9497 × 10 ⁹	1.8889 × 10 ¹⁰	1.1173 × 10 ⁵	8.9498 × 10 ⁹	1.8889 × 10 ¹⁰
1/6	10 ⁻⁶	10 ³⁶	10 ⁻⁹	1.1173 × 10 ⁶	8.9498 × 10 ¹¹	1.8889 × 10 ¹²	1.1173 × 10 ⁶	8.9498 × 10 ¹¹	1.8889 × 10 ¹²

In the small $\tilde{\sigma}$ limit, the relevant root for \tilde{k}^2 is determined, at leading order, by balancing the first and second terms in (61), giving

$$\tilde{k}^2 = \tilde{k}_{oc}^2 = \left(\frac{\tilde{\sigma}^2 \tilde{T}}{2} \right)^{1/3}. \quad (63)$$

The final two terms in expression (60) are then dominant, giving

$$\tilde{R}_c^{(o)} = \frac{2\tilde{\sigma}^2 \tilde{T}}{\tilde{k}_{oc}^2} + 2\tilde{k}_{oc}^4 = 3 \left(2\tilde{\sigma}^4 \tilde{T}^2 \right)^{1/3}. \quad (64)$$

The scaled frequency, using Eq. (62), is given by

$$\tilde{\omega}_c^2 = \left(2\tilde{\sigma}^4 \tilde{T}^2 \right)^{1/3}. \quad (65)$$

Reverting to the unscaled variables, all the Γ dependence vanishes, and we simply obtain

$$k_{oc}^2 = \left(\frac{\sigma^2 T}{2} \right)^{1/3}, \quad \text{with} \quad \omega_c^2 = \left(2\sigma^4 T^2 \right)^{1/3} \quad \text{and} \quad R_c^{(o)} = 3 \left(2\sigma^4 T^2 \right)^{1/3}. \quad (66)$$

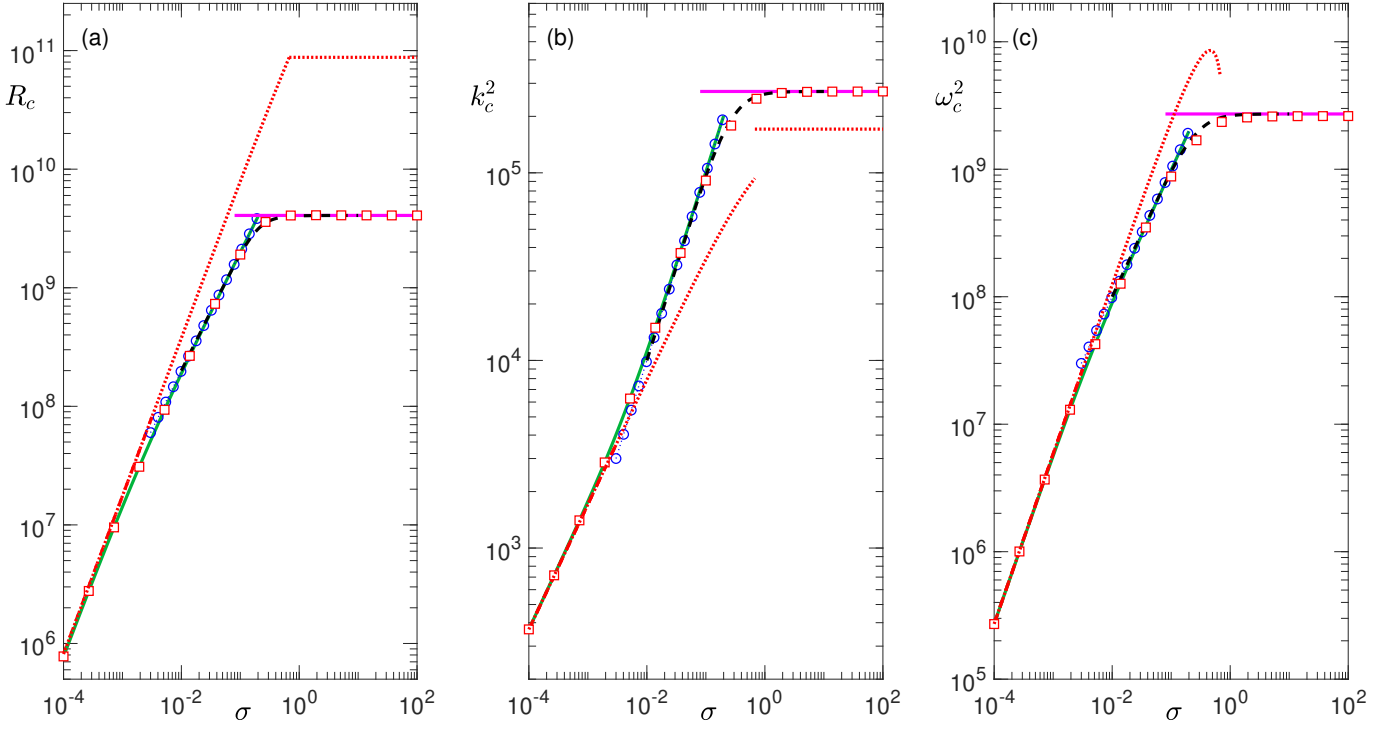


FIG. 5: (a) R_c , (b) k_c^2 and (c) ω_c^2 as functions of σ for the case of $\Gamma = 10^{-4}$, $T = 10^{16}$ (i.e. $\lambda = 1/4$); the onset of instability is oscillatory for all σ . The magenta lines denote the asymptotic expressions (46); the black dashed lines are the expressions (50) (for (a)), (51) (for (b)) and (52) (for (c)), with the respective limiting values (57), (54) and (55) shown by the blue dotted lines with circle markers; the green lines are given by (60) (for (a)), (61) (for (b)) and (62) (for (c)), with the respective limiting expressions (66) shown as red dashed lines. Numerical results of the full system are shown as squares with red edges. For comparison, the red dotted lines denote R_c , k_c^2 and ω_c^2 for the classical problem; here the onset of instability is oscillatory for $\sigma < \sigma_c$ and steady for $\sigma > \sigma_c$.

Thus, in this regime of very small σ , the M-C effect has no influence; the last vestiges of the M-C effect are contained in the final term in (61). Expressions (66) are therefore the small σ limits of the classical expressions (26), valid for $\sigma^2 T \gg 1$. For yet smaller σ , the M-C influence, already negligible in expressions (66), is diminished further. Thus, on descending into the regimes with $\sigma^2 T = O(1)$ and then $\sigma^2 T \ll 1$ (both with $T \gg 1$, $\sigma \ll 1$), the relevant criteria are those discussed in Sec. IID for the classical problem. It is noteworthy that for $\sigma^2 T$ to be $O(1)$, σ has to be incredibly small, with $\sigma = O(\Gamma^{1/\lambda})$.

C. The effect of the Prandtl number on the stability boundary

Having explored the stability boundary for $\sigma \gtrsim 1$ in Sec. IVA and for small σ in Sec. IVB, we can now piece together the critical Rayleigh number and optimal wavenumber across an extended range of σ . Figure 5 depicts R_c , k_c^2 and ω_c^2 versus σ over the range $10^{-4} \leq \sigma \leq 10^2$ for $\Gamma = 10^{-4}$ and $T = 10^{16}$ ($\lambda = 1/4$); thus, even the smallest value of σ shown satisfies $\sigma^2 T \gg 1$. The form of the plot is representative of all values of $\lambda < 1/3$. The asymptotic expressions (46), (50)–(52) and (60)–(62) are plotted, together with the limiting expressions (57) and (66); the smooth transition between the various regimes is exhibited clearly. Numerical solutions from the full system are also shown; these are in excellent agreement with the asymptotic results. For comparison, R_c and k_c^2 for the classical ($\Gamma = 0$) problem at the same value of T are also shown. As discussed in Sec. IID, when there is no M-C influence, the onset of instability is oscillatory for $\sigma < \sigma_c = 0.6766$ and steady for $\sigma > \sigma_c$. For the parameters considered here, although M-C effects are becoming insignificant for the smallest values of σ shown ($\sigma = O(10^{-4})$), the M-C effect is clearly destabilising for $\sigma \gtrsim O(10^{-3})$; moreover, as discussed above, it leads to an oscillatory onset of instability for all σ and an increase in the wavenumber and frequency of the preferred mode.

V. CONCLUSION

In this paper, we have considered the effects of small Maxwell-Cattaneo (M-C) corrections to the linear stability of rapidly rotating Boussinesq convection in a plane layer heated from below. The work builds on earlier papers (refs. [35, 38]), which consider the M-C effect in magnetoconvection and double-diffusive convection, respectively. The principal conclusion is that when the Taylor number T is large, but the (small) M-C effect, represented by the parameter Γ , is large enough that $\Gamma > O(T^{-\lambda})$ for $\lambda \leq 1/3$, then the stability boundary differs significantly from the classical case ($\Gamma = 0$); in the latter, it is known that if T is sufficiently large and the Prandtl number $\sigma < 1$, then oscillatory convection is possible, while oscillations are preferred for $\sigma < 0.6766$ [40]. The effect of the M-C terms is negligible for $\lambda > 1/3$. For $\lambda = 1/3$, oscillations can be preferred for values of T of order Γ^{-3} , even for large values of σ , while the critical values of the Rayleigh number and wave number remain, at $O(T^{2/3})$ and $O(T^{1/6})$, similar to those for the classical problem. At very small values of σ we find that the critical values of R and k^2 are close to those for the classical problem: oscillations are always preferred.

For $\lambda < 1/3$ oscillations are always preferred; indeed, the critical values of R for oscillatory onset are now asymptotically smaller than that for steady convection, so oscillations are strongly preferred for small Γ while the critical wavenumbers now increase with Γ . The results exhibit the same balance of terms for values of $\sigma \geq O(1)$, but the dominant balances change considerably as σ becomes small and there are several distinct small- σ regimes to be analysed. When σ is sufficiently small, M-C effects become negligible.

The M-C effect, represented by Γ , is typically very small, as discussed in [35], though it is hard to find good data on relaxation times for terrestrial fluids. How large does Γ have to be before there is a discernible effect on the onset of convection? From the analysis presented here, we expect significant effects when $\Gamma T^{1/3}$ is of order unity or greater. As noted in the introduction, T can be as large as 10^{30} in the Earth's outer core, so it seems plausible to expect M-C effects to occur there. In the laboratory, assuming scales of order 2 metres, angular velocity of 2000 rpm and kinematic viscosity of $10^{-6} \text{m}^2 \text{s}^{-1}$, T could be as large as 10^{14} ; it thus seems possible, depending on the nature of the fluid, that in this case also we can find regimes where M-C effects should be taken into account.

The analysis of the paper assumes that the convection is in what one might call the fundamental vertical mode, with, for example, the vertical velocity proportional to $\sin z$. There are in fact an infinite number of solutions with the vertical velocity $\propto \sin mz$ for any integer m . Because the great majority of the modes described in the paper have large critical horizontal wavenumbers, the value of m does not appear at leading order in the results — or, to put it another way, the vertical structure of the convection is not determined at leading order. In the few cases where the critical wavenumber is of order unity, it can be verified that $m = 1$ gives the smallest critical Rayleigh number.

The paper addresses only the case of stress-free velocity boundary conditions. Any laboratory experiments would involve at least one rigid boundary, so it is reasonable to ask what difference in the results might be expected. In fact, at large Taylor number, as in the case of large Chandrasekhar number in magnetoconvection [35], the primary balance in the interior is unaffected by the velocity boundary conditions at leading order, the no-slip condition being passively accommodated by narrow Ekman layers. We therefore expect the results obtained here to apply at leading order irrespective of the velocity boundary conditions.

It is well known that there is a broad analogy between the rotating and magnetic convection problems, in that the dispersion relations for a fixed wavenumber have a very similar form; however, because of different wavenumber dependencies, the relations defining the optimal wavenumbers in the two problems (for both steady and oscillatory convection) are rather different. The same remains true when M-C effects are included.

Finally, it should be noted that the analysis in this paper assumes the Boussinesq approximation: thus Mach numbers are assumed small and the fluid is taken as incompressible. Equivalently, the sound speed is taken as effectively infinite. In real fluids there will be high frequency sound waves at any given velocity scale, and while the structure of these waves (almost irrotational) and the M-C induced oscillations (almost solenoidal) are very different, and the modes are likely to interact only weakly, it would nonetheless be of interest to extend the analysis of the present paper to include the effects of weak compressibility to see if there is any material change in the general conclusions reached here.

ACKNOWLEDGMENTS

We are grateful to the referees for their helpful comments on the paper.

[1] J. C. Maxwell, On the dynamical theory of gases, Phil. Trans. R. Soc. Lond. **157**, 49 (1867).

- [2] C. Cattaneo, Sulla conduzione del calore, *Atti Mat. Fis. Univ. Modena* **3**, 83 (1948).
- [3] J. G. Oldroyd, On the formulation of rheological equations of state, *Proc. R. Soc. Lond. Ser. A* **200**, 523 (1950).
- [4] N. Fox, Low temperature effects and generalized thermoelasticity, *IMA J. Appl. Maths.* **5**, 373 (1969).
- [5] M. Carrassi and A. Morro, A modified Navier-Stokes equation, and its consequences on sound dispersion, *Nuovo Cimento B Serie* **9**, 321 (1972).
- [6] A. Barletta and E. Zanchini, Unsteady heat conduction by internal-energy waves in solids, *Phys. Rev. B* **55**, 14208 (1997).
- [7] B. Straughan and F. Franchi, Bénard convection and the cattaneo law of heat conduction, *Proc. R. Soc. Edin.* **96**, 175 (1984).
- [8] G. Lebon and A. Clout, Bénard-Marangoni instability in a Maxwell-Cattaneo fluid, *Phys. Lett. A* **105**, 361 (1984).
- [9] B. Straughan, Oscillatory convection and the Cattaneo law of heat conduction, *Ric. di Mat.* **58**, 157 (2009).
- [10] B. Straughan, Thermal convection with the Cattaneo-Christov model, *Int. J. Heat Mass Transf.* **53**, 95 (2010).
- [11] D. F. Stranges, R. E. Khayat, and B. Albaalbaki, Thermal convection of non-Fourier fluids. Linear stability, *Int. J. Therm. Sci.* **74**, 14 (2013).
- [12] D. F. Stranges, R. E. Khayat, and J. deBruyn, Finite thermal convection of non-Fourier fluids, *Int. J. Therm. Sci.* **104**, 437 (2016).
- [13] J. J. Bissell, On oscillatory convection with the Cattaneo-Christov hyperbolic heat-flow model, *Proc. R. Soc. Lond. Ser. A* **471**, 20140845 (2015).
- [14] I. A. Eltayeb, Convective instabilities of Maxwell-Cattaneo fluids, *Proc. R. Soc. Lond. Ser. A* **473**, 20160712 (2017).
- [15] B. Straughan, Porous convection with local thermal non-equilibrium temperatures and with Cattaneo effects in the solid, *Proc. R. Soc. Lond. Ser. A* **469**, 20130187 (2013).
- [16] S. Haddad, Thermal instability in Brinkman porous media with Cattaneo-Christov heat flux, *Int. J. Heat Mass Transf.* **68**, 659 (2014).
- [17] J. J. Vadasz, S. Govender, and P. Vadasz, Heat transfer enhancement in nano-fluids suspensions: Possible mechanisms and explanations, *Int. J. Heat Mass Transf.* **48**, 2673 (2005).
- [18] P. Vadasz, Heat conduction in nanofluid suspensions, *ASME J. Heat Transf.* **128**, 465 (2006).
- [19] D. Jou, A. Sellitto, and F. X. Alvarez, Heat waves and phonon-wall collisions in nanowires, *Proc. R. Soc. Lond. Ser. A* **467**, 2520 (2011).
- [20] G. Lebon, H. Machrafi, M. Grmela, and C. Dubois, An extended thermodynamic model of transient heat conduction at sub-continuum scales, *Proc. R. Soc. Lond. Ser. A* **467**, 3241 (2011).
- [21] H. W. Liepmann and G. A. Laguna, Nonlinear interactions in the fluid mechanics of helium II, *Ann. Rev. Fluid Mech.* **16**, 139 (1984).
- [22] R. J. Donnelly, The two-fluid theory and second sound in liquid helium, *Physics Today* **62**, 34 (2009).
- [23] H. Liu, M. Bussmann, and J. Mostaghimi, A comparison of hyperbolic and parabolic models of phase change of a pure metal, *Int. J. Heat Mass Transf.* **52**, 1177 (2009).
- [24] A. Miranville and R. Quintanilla, A generalization of the caginalp phase-field system based on the cattaneo law., *Nonlinear Anal., Real World Appl.* **71**, 2278 (2009).
- [25] S. Rastear, Hyperbolic heat conduction In pulsed laser irradiation of tissue, in *Thermal and Optical Interactions with Biological and Related Composite Materials*, Vol. 1064, edited by M. J. Berry and G. M. Harpole (SPIE, 1989) pp. 114 – 117.
- [26] W. Kaminski, Hyperbolic heat conduction equation for materials with a non-homogeneous inner structure, *ASME J. Heat Transf.* **112**, 555 (1990).
- [27] K. Mitra, S. Kumar, A. Vedavarz, and M. K. Moallemi, Experimental evidence of hyperbolic heat conduction in processed meat, *ASME J. Heat Transf.* **117**, 568 (1995).
- [28] Y. Dolak and T. Hillen, Cattaneo models for chemosensitive movement - numerical solution and pattern formation (vol 46, pg 153, 2003), *J. Math. Bio.* **46**, 460 (2003).
- [29] A. Saidane, S. Aliouat, M. Benzohra, and M. Ketata, A transmission line matrix (tlm) study of hyperbolic heat conduction in biological materials, *J. Food Eng.* **68**, 491 (2005).
- [30] W. Dai, H. Wang, P. Jordan, R. Mickens, and A. Bejan, A mathematical model for skin burn injury induced by radiation heating, *Int. J. Heat Mass Transf.* **51**, 5497 (2008).
- [31] E. Barbera, C. Curro, and G. Valenti, A hyperbolic reaction-diffusion model for the hantavirus infection, *Math. Meth. Appl. Sci.* **31**, 481 (2008).
- [32] M. M. Tung, M. Trujillo, J. A. Lopez Molina, M. J. Rivera, and E. J. Berjano, Modeling the heating of biological tissue based on the hyperbolic heat transfer equation, *Math. Comp. Mod.* **50**, 665 (2009).
- [33] L. Herrera and N. Falcón, Heat waves and thermohaline instability in a fluid, *Phys. Lett. A* **201**, 33 (1995).
- [34] J. J. Bissell, Thermal convection in a magnetized conducting fluid with the Cattaneo-Christov heat-flow model, *Proc. R. Soc. Lond. Ser. A* **472**, 20160649 (2016).
- [35] I. A. Eltayeb, D. W. Hughes, and M. R. E. Proctor, The convective instability of a Maxwell-Cattaneo fluid in the presence of a vertical magnetic field, *Proc. R. Soc. Lond. Ser. A* **476**, 20200494 (2020).
- [36] P. M. Jordan, Growth and decay of shock and acceleration waves in a traffic flow model with relaxation, *Physica D* **207**, 220 (2005).
- [37] C. I. Christov, On frame indifferent formulation of the Maxwell-Cattaneo model of finite-speed heat conduction, *Mech. Res. Commun.* **36**, 481 (2009).
- [38] D. W. Hughes, M. R. E. Proctor, and I. A. Eltayeb, Maxwell-Cattaneo double-diffusive convection: limiting cases, *J. Fluid Mech.* **927**, A13 (2021).

- [39] S. Chandrasekhar, The instability of a layer of fluid heated below and subject to Coriolis forces, Proc. R. Soc. Lond. Ser. A **217**, 306 (1953).
- [40] S. Chandrasekhar, *Hydrodynamic and Hydromagnetic Stability* (Clarendon Press, Oxford, 1961).
- [41] G. Veronis, Cellular convection with finite amplitude in a rotating fluid, J. Fluid Mech. **5**, 401 (1959).
- [42] N. O. Weiss, Convection in the presence of restraints, Phil. Trans. R. Soc. Lond. Ser. A **256**, 99 (1964).
- [43] R. C. Kloosterziel and G. F. Carnevale, Closed-form linear stability conditions for rotating Rayleigh-Bénard convection with rigid stress-free upper and lower boundaries, J. Fluid Mech. **480**, 25 (2003).